Positronium formation via excitonlike states on Si and Ge surfaces

D. B. Cassidy, T. H. Hisakado, H. W. K. Tom, and A. P. Mills Jr.

Department of Physics and Astronomy, University of California, Riverside, California 92521-0413, USA

Recent experiments combining lifetime and laser spectroscopy of positronium (Ps) show that these atoms are emitted from p-Si(100) at a rate that depends on the sample temperature, suggesting a thermal activation process, but with an energy that does not, precluding direct thermal activation as the emission mechanism. Moreover, the amount of Ps emitted is substantially increased if the target is irradiated with 532 nm laser light just prior to the implantation of the positrons. Our interpretation of these data was that the Ps was emitted via an excitonlike positron-electron surface state, not dissimilar to an electronic surface exciton observed on Si in two-photon photoemission measurements. The hypothesis that this state may be populated by electrons from one of the occupied electronic surface states, either thermally or by laser excitation, is consistent with our observations and suggests that one should expect a high Ps yield at room temperature from an n-doped Si(100) sample, since in this case the same surface states will already be occupied. Here we present data obtained with an n-Si(100) target that supports our model, and also reveals the unexpected result that the kinetic energy of Ps emitted from this material actually *decreases* when it is heated, an effect we attribute to shifts in the surface energy levels due to the presence of a high density of thermally generated electrons. We show data obtained with a Ge(100) sample that corroborate the idea that the effects we observe are related to surface electron states, and hence should occur for any indirect-band-gap semiconductor with dangling-bond states. Our model is further confirmed by the observation that the Ps yield from p-Si depends linearly on the surface density of the implanted positrons due to the effects of electron-hole pairs created as the positrons slow down.

I. INTRODUCTION

Positronium (Ps) is a hydrogenlike bound state between a positron and an electron.[1,2] This atomic system [3] is metastable, in that the particle and antiparticle will eventually annihilate each other, producing γ rays. For positronium in its ground state, the annihilation rate depends on the relative spin states of the electron and positron: if the spins are parallel (triplet states) the mean lifetime is relatively long (142 ns) whereas the antiparallel (singlet) configuration is short lived (0.125 ns). Despite its relatively short lifetime, Ps can still be used in a wide array of experiments, including precision laser spectroscopy,[4] Ps ion[5] or molecule[6] formation, Ps-atom scattering cross section measurements,[7] studies of defects,[8] thin film polymers,[9] surface magnetism,[10] electronic densities of states,[11] quantum sticking,[12] and fundamental symmetry tests.[13]

Positronium may be produced through various different mechanisms, all of which involve irradiating some material (which in practice can be almost anything) with positrons. The first observation of Ps by Deutsch in 1951 [14] used fast positrons emitted by a ^{22}Na source interacting with N_2 and NO gases. A similar technique using a moderated positron beam and a gas cell is still used today to produce tunable Ps beams for atomic physics scattering measurements.[7,15]

For many experiments, however, the production of Ps is more efficiently achieved by implanting slow positrons into solid materials.[16,17] In this case most of the positrons rapidly lose their kinetic energy down to a few eV (in $\sim$1 ps or less[18]) and approach the ambient sample temperature, whereupon they may capture an electron directly to form Ps. In an insulator this may occur in the bulk material,[19,20] while in conductors or semiconductors Ps may only be formed on surfaces; bulk Ps is unbound because of screening effects in metals,[21] or

likely exists as a weakly bound excitonlike state in some semiconductors.[22]

The existence of positron surface states on numerous conductors and semiconductors, and their role in the production of vacuum Ps, has been understood for some time.[16,23] Usually a surface positron is thought to reside in a relatively shallow surface potential well caused by its image charge and may form Ps via a thermal activation process wherein the positron and an electron from the conduction band are emitted together in the form of a Ps atom following a random thermal kick. This results in the production of thermal Ps in vacuum[24] and has been the method used to obtain thermal Ps for many experiments.[16]

Recently there has been a growing interest in using certain porous materials[25] to produce Ps in vacuum.[26–28] Ps may be formed from such materials quite efficiently (reported Ps fractions range from approximately 20% to 60%). Positronium atoms are emitted into the voids of such materials from the bulk by work-function emission,[19] which is largely independent of the sample temperature. However, this does mean that such Ps will be initially hot [$\sim$1 eV (Ref. 20)] and must cool via collisions with the internal surfaces, which can lead to annihilation. Thus, the colder the emitted Ps, the less there will be, and the longer it will take to leave the sample.[29] Since Ps emission times can be comparable to the lifetime in the pores, which may be tens of nanoseconds or more,[30] Ps produced by this method may not be optimal for some experiments (for example, excitation with laser pulses that are much shorter than the Ps emission time). Moreover, such materials can be highly susceptible to laser damage even at room temperature;[31] this situation is likely to be worse at lower temperatures,[32] and may even lead to significant damage being created by the incident positron beam if it is intense enough.[33]

In this paper we describe experiments in which an intense pulsed positron beam[34] is used to produce short pulses of Ps. Lifetime and laser spectroscopy has revealed that the emission of Ps from the surface of *p*-Si(100) does not, for the most part, occur via the usual channels for metals or semiconductors[35] described above (i.e., direct capture of electrons by energetic positrons or thermal desorption of Ps from a positronic surface state[24]). Rather, Ps from this material is mostly emitted via the formation of an intermediate surface electron-positron bound state that appears to be analogous to the surface exciton (that is, an electron bound to a hole in the surface band) observed by Weinelt *et al.*[36] The surface excitons are formed when electrons are excited from the valence to the conduction band and then become captured in dangling-bond surface states, from whence they form surface excitons by becoming bound to surface holes.[36] However, if there is a positron present on the surface, as may be the case just after the implantation of a positron pulse, then these electrons may form positronium via a similar mechanism. It turns out that such Ps is emitted spontaneously, with a constant energy of $\sim$0.16 eV,[35] that is determined by the particular electron and positron energy levels of the system.

The formation of Ps via this mechanism depends on the availability of surface electrons, which may be produced either thermally[35] or by laser irradiation.[36] The former process involves the thermal activation of electrons to surface states, the existence of which is dependent on the presence of a positron, which means that the temperature dependence of Ps emission from Si looks almost identical to thermal activation curves obtained from metal samples.[37] Indeed, it is only when both the Ps yield and emission energy are measured that the actual mechanism becomes clear. Since electron-hole (*e-h*) pairs are produced by above-band-gap light, the Ps yield from Si can be increased by laser irradiation instead of heating.[38] We show here that *e-h* formation by the slowing down of the incident positrons may also populate the same electronic states, and that as a result the amount of Ps emitted from a *p*-Si surface depends on the incident positron beam characteristics in an unusual way. That is, while the Ps fraction usually depends on the beam energy only via the positron implantation depth (and subsequent diffusion back to the surface[39,40]), in the case of *p*-Si this dependence is modified to reflect the formation of *e-h* pairs, which will increase in number with the beam energy, but at the same time tend to decrease in effectiveness due to the lateral spreading associated with diffusion to the surface from increasing depths. Moreover, if the positron beam density is high enough then *e-h* pairs produced by one positron may affect the rate at which another positron is able to form Ps, resulting in a Ps fraction that depends on the beam density. Here we present data that demonstrate these effects, and also data obtained with *n*-doped Si and Ge samples. The latter corroborate our model of Ps formation via excitonlike surface positronium states, insofar as they are different from the *p*-Si samples already studied in a manner fully consistent with the different Fermi energies in these materials.

II. EXPERIMENTAL METHODS

A. Positron accumulator

The positron accumulator used for this work, described in more detail elsewhere,[34] utilizes a slow positron beam

produced from an encapsulated ^{22}Na radioactive source and a neon moderator[41] in the standard way.[42] With a 50 mCi source, we obtained a dc positron beam with an intensity of $\sim$1.5 $\times$ 10^7 s^{-1}. With our current source strength of $\sim$12 mCi we have $\sim$2 $\times$ 10^6 s^{-1}. Although the latter rate is not quite optimal (moderator efficiencies of $\sim$1% have been measured), it is obtained under very stable conditions, which is advantageous for the kind of experiments we describe here.

The dc beam enters a two-stage Surko trap[43,44] running at 2 Hz whose output is stored in an accumulator. When a sufficient number of positrons have been captured, single-component plasmas[45] are produced whose density may be precisely controlled using the "rotating-wall" (RW) technique.[46,47] This is a method wherein the application of a suitably phased potential is applied to segmented electrodes, resulting in a rotating transverse dipolar electric field that applies a torque to the plasma. Since the angular momentum of the plasma is conserved,[48] this causes radial compression, increases the density, and improves the confinement properties of the positron plasma.

We operate our RW compression in what is known as the strong-drive regime,[49,50] which means that the plasma density almost exactly follows the applied RW drive frequency. Unfortunately, this only occurs up to some maximum drive frequency value, which for us is $\sim$12 MHz,[51] although higher values (up to 50 MHz) have been observed in a similar system.[52] The reasons why compression fails above a certain frequency are not presently known. Some possibilities are transmission problems of the RW signal, a high density of zero-frequency modes[49] induced by electrostatic asymmetries, or perhaps even a fundamental property of gas-cooled single-component plasmas.[53] In our experiments the beam is implanted into a target with a central areal density given by

$$n_{2D} = \left[\frac{f_{RW}}{12\text{ MHz}}\right] \times \left[\frac{B_T}{2.3\text{ T}}\right] \times 9.4 \times 10^{10}\text{ cm}^{-2}, \quad (1)$$

where f_{RW} is the rotating-wall drive frequency and B_T is the magnetic field at the target. Note that the beam density on target is independent of the accumulator magnetic field, so long as the plasma compression remains in the strong-drive regime. This is simply due to the fact that the reduction of the plasma density in the accumulator for a lower magnetic field is exactly cancelled out by the corresponding increase in the beam compression when it enters the target magnetic field.[54]

The positron plasmas are ejected from the accumulator with a prebuncher, which is a suddenly applied parabolic voltage distribution (300 V maximum) ramped across the electrode structure. This produces a pulse whose time width depends strongly on the plasma space-*c*harge potential, and thus on the number of positrons. For most of the experiments described here the number of positrons was around 2 $\times$ 10^7, which would result in pulses of $\sim$30 ns, full width at half maximum (FWHM) at the target position. However, these pulses are further compressed in time to $\sim$1 ns (FWHM) using a high-voltage electrostatic buncher just before the target.[34,54] The full buncher voltage is $\sim$1.5 kV and results in a minimum beam energy of around 0.75 kV and an energy spread of $\sim$1 keV.

B. Single-shot lifetime measurements

Following positron implantation into the target, the resulting annihilation radiation is detected with a $PbWO_4$ scintillator and fast phototube,[55] and single shot lifetime spectra are generated.[56] These are used to determine the delayed fraction f_d, which we define as the fraction of the spectrum in the interval of 50 to 300 ns divided by the total, as shown in Fig 1. This region is chosen to accommodate the particular features of our detector, namely, the $PbWO_4$ scintillator decay time (~ 15 ns) and an ion feedback pulse in the photomultiplier tube (PMT) at about 350 ns. For different detectors different regions would be used. For example, if timing information were needed we might use a PbF_2 Cherenkov radiator and/or a fast microchannel plate PMT. More details about detectors suitable for single-shot lifetime measurements are given in Ref. 54.

We can relate the total Ps fraction f_{Ps} to the measured delayed fraction in the following way. We assume that the prompt part of the detector response, $V_p(t)$, may be modeled using a single exponential with amplitude $(1-a)$ and lifetime $\tau_1 = 17$ ns, which is identical with the detector time resolution[55]:

$$V_p(t) = (1-a)\tau_1^{-1}\exp\{-t/\tau_1\}\theta(t), \qquad (2)$$

where $\theta(t)$ is the unit step function. The total fraction of positrons that form positronium, the Ps fraction f_{Ps}, can be 1 at most and the fraction of positrons that form Ps in the triplet state is a, so $f_{Ps} = \frac{4}{3}a$. The measured delayed component is taken to be a single exponential with amplitude a and lifetime $\tau_2 = 95$ ns and relative efficiency η for detecting 3γ vs 2γ annihilations, folded with the system resolution given by the prompt curve $V_p(t)$:

$$
\begin{aligned}
V_d(t) &= \int_0^\infty \eta a\tau_2^{-1}\exp\{-t'/\tau_2\}\theta(t')\tau_1^{-1} \\
&\quad \times \exp\{-(t-t')/\tau_1\}\theta(t-t')dt' \\
&= \eta a(\tau_2-\tau_1)^{-1}[\exp\{-t/\tau_2\} - \exp\{-t/\tau_1\}]\theta(t) \geqslant 0.
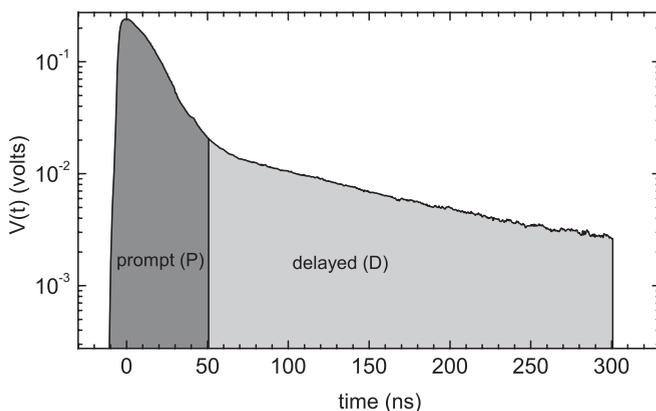\end{aligned}
\qquad (3)
$$

FIG. 1. Example of a single-shot lifetime spectrum taken using a $PbWO_4$ scintillator and with a p-Si(100) target. The vertical scale is the absolute value of the output voltage from the photomultiplier that is coupled to the scintillator. The prompt (P) and delayed (D) areas are indicated by the shaded regions. The delayed fraction, as defined in the text, is given by $f_d = D/(D+P)$.
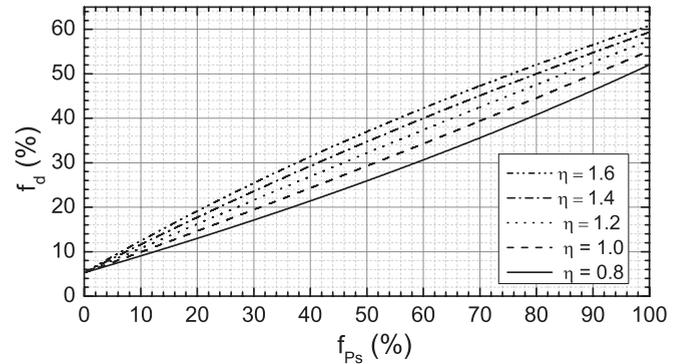

FIG. 2. Relation between the positronium fraction f_{Ps} and the delayed fraction f_d for different values of the 2γ:3γ detection efficiency ratio η, as described in the text.

We may now compute the delayed fraction using this exponential response model for the prompt and delayed components:

$$
\begin{aligned}
f_d &= \frac{\int_{50}^{300}[V_p + V_d]dt}{\int_0^{300}[V_p + V_d]dt} \\
&\approx \frac{[(1-a)(\tau_2-\tau_1)-a\eta\tau_1]e^{-50/\tau_1} + a\eta\tau_2[e^{-50/\tau_2}-e^{-300/\tau_2}]}{(1-a)(\tau_2-\tau_1)-a\eta\tau_1 + a\eta\tau_2[1 - e^{-300/\tau_2}]}.
\end{aligned}
\qquad (4)
$$

Here we have neglected terms proportional to e^{-300/τ_1}. When $a = 0$, we have a minimum value of the delayed fraction $f_{d,\min} = \exp\{-50/\tau_1\} \approx 0.053$, in agreement with the actual background component $f'_{d,b} \approx 0.04$ which we observe in all our lifetime spectra. The agreement is slightly fortuitous because the real single-shot lifetime spectrum of Fig. 1 is not precisely a sum of two exponentials, and part of the background may be due to a fluorescence tail on the prompt peak, which may be a characteristic of the $PbWO_4$ scintillator or perhaps even of the PMT cathode window. Figure 2 shows the delayed fraction expected as a function of the positronium fraction for various values of the 3γ:2γ detection efficiency η. As a rough approximation one may convert f_d (%) values to Ps fractions (%) via $f_{Ps} \approx 2(f_d - 5)$. Note that $\eta = 1$ would be expected for an ideal version of our experiment in which the total energies of two- and three-photon decays both contribute equally to the detector response. A smaller value of η would result from the preferential absorption of the lower-energy 3γ-decay photons in the chamber walls and surrounding materials, and also from the directionality of the 3γ decays in a strong magnetic field, which does not favor detection of $|m| = 1$ ortho-Ps decays in a plane perpendicular to the magnetic field direction.[57] A larger value of η would result if the total number of photons were an important factor, for example due to preferential scattering of the lower-energy 3γ annihilation photons into the detector.

C. Laser systems

The laser systems used here are similar to those described previously,[29] but with a few modifications. A schematic of the most recent optical layout of the laser system is shown in Fig. 3. A Q-switched Nd:YAG laser with phase-matched

FIG. 3. Configuration of the laser systems. Here CLRS refers to the closed-loop rotational stage used for wavelength tuning, DGS to the diffraction grating spectrometer, and TC to the target chamber where the laser-Ps interactions took place. Q, quad detector for maintaining beam alignment; SM, stepper motor; PG, photo gate.

second- and third-harmonic generation crystals was used to provide 532 and 355 nm light, the latter being used to pump a dye laser (LD 489 dye) with the grating set at first-order Littrow to produce broadband 486 nm pulses.

The 486 nm output was frequency doubled in a type-I phase-matched β barium borate (BBO) crystal to produce ~4-ns-duration 1 mJ pulses at 243 nm. The dye laser wavelength and the phase-matching angle of the BBO were varied using a computer-controlled stepper motor that optimized the phase matching at each wavelength.

The 243 nm wavelength and bandwidth were determined by characterizing the 486 nm pulse split off just after the frequency-doubling crystal. The center wavelength was determined using a Bristol 821 pulsed laser wavelength meter. For these broadband pulses (~90 GHz), the center frequency had an absolute accuracy of ± 6 GHz at 486 nm and a shot-to-shot variation of 7 GHz due to the fluctuations in the distribution of energy in the cavity modes within the 90 GHz envelope. The bandwidth was determined using a SPEX 0.75 m diffraction grating spectrometer operated at $f/8$ with a 1200 line/mm grating in second order with a CCD array at the exit slit. Wavelength differences on the spectrometer were calibrated using multiple lines from a mercury light source which was made to copropagate with the dye laser output to better than 50 μrad. The 486-nm-pulse bandwidth envelope was fitted to a Gaussian profile and measured to be 90 ± 10 GHz (FWHM), where the variation from shot to shot was also consistent with the energy distribution between cavity modes. The acceptance bandwidth of the BBO was 500 GHz (FWHM), and the phase-matching angle of the BBO crystal was computer controlled to track the dye laser so the second-harmonic output frequency can be considered to be

ideally doubled over the 90 GHz bandwidth. The 243 nm pulse was then calculated to have a 130 ± 14 GHz (FWHM) average linewidth with center frequency absolute uncertainty of ± 12 GHz.

For some of our experiments we used a 532 nm light pulse to generate Ps in the target and tunable UV light around 243 nm to probe the $1S$-$2P$ transition of the resulting Ps atoms. Since the 532 nm pulse had to be incident at independently variable times relative to the Ps pulse, we used a second Q-switched Nd:YAG laser (Surelite I-20) outfitted with a phase matched Potassium dideuterium phosphate (KD*P) crystal to provide up to 110 mJ, ~7-ns-duration 532 nm pulses.

The positron and laser pulses were synchronized using a photomultiplier tube with a plastic scintillator, arranged so that the γ-ray flash from the positron dump had a path length from the detector to the target similar to that of the laser light, which was admitted to the scintillator crystal through a black cloth covering a pinhole in the light-tight PMT enclosure.[58]

D. Sample preparation

In this paper we present data for p-Si(100) and n-Si(100) as well as n-Ge(100). The doping type of the n-Ge(100) sample was determined by measuring the sign of the Hall effect, and its room temperature resistivity was determined to be $18 \pm 1 \, \Omega$ cm by van der Pauw measurements on a $19 \times 21 \times 0.45$ mm^3 sample from the same batch as the one for our Ps experiments. The doping is equivalent to ~5×10^{13} Sb/cm^{-3},[59] and is not very different from that of undoped Ge, which has a room temperature resistivity of 47 Ω cm, equivalent to ~2.4×10^{13} Sb/cm^{-3}.

We shall discuss data obtained from two p-Si samples that were cleaned in slightly different ways. As described in Ref. 35, the first p-Si(100) target had dimensions $10 \times 10 \times 0.34$ mm^3 with a resistivity we measured to be 2.7 Ω cm at 300 K, corresponding to $(5.2 \pm 0.2) \times 10^{15}$ boron atoms cm^{-3}. The sample surface was prepared by dipping in 100% ethanol, followed by dipping in ~2–4% HF for ~1 min to remove the surface oxide, as evidenced by the surface becoming hydrophobic. The sample was then rinsed by dipping in distilled water, leaving no observable trace of water on the surface, and evacuated in the target chamber within ~5 min. This preparation can produce a hydrogen-terminated surface,[60] which leads to a (2 × 1) reconstructed dangling-bond surface at 300 K after the hydrogen has been desorbed by heating to around 1000 K.[61] While the vacuum system was baked at a temperature of ~200 °C for 36 h, the sample was outgassed at 300 °C, and then, following bakeout, gradually heated to 1000 K. During the heating process, the positronium formation fraction increased, presumably due to the desorption of hydrogen, with the surface eventually becoming stable under repeated thermal cycling from 300 to 1000 K.

The second boron-doped p-Si(100) sample was cleaved from one of the same batch of wafers as the first. It was prepared without dipping to reduce any contamination picked up from liquid surfaces. To completely remove the surface layer of oils and dust, the Si surface was first wiped with a tissue dipped in 100% ethanol and then blown dry with a canister duster. The surface was then etched with a drop of ~10%

HF acid using a pipette. After application of the drop, it was observed to spread instantly over the entire surface and then quickly bead up into a single large drop, indicating the removal of the oxide layer. The liquid was removed by sucking it up into the pipette after about 30 s. The surface was then rinsed with a similarly applied and removed drop of distilled water, and any remaining drops on the back were blown off with the duster. The phosphorus-doped n-Si(100) sample (manufacturer-stated resistivity 1–10 Ω cm) was cleaned in the same way.

The Ge(100) cleaning procedure followed the prescription of Sun *et al.*;[62] oils and particles were removed using a lint-free wiper wetted with pure ethanol.[63] The sample was then dipped in distilled water for 30 s to dissolve the native oxide before being dipped in ∼10% H_2O_2 for 30 s to grow a fresh oxide layer, and was then immersed in ∼10% HCl for ∼10 min, presumably leaving a mono- and dichloride surface [since there are two dangling bonds for each Ge(100) surface atom]. The sample was blown dry before insertion into the vacuum system. Before our experiments were conducted, the Ge sample was heated to 650 K to desorb chlorine.

All samples were placed into the vacuum chamber within a few minutes of cleaning. The chamber was then pumped out to a pressure $<1 \times 10^{-7}$ Torr within ∼5 min. After baking, the base pressure of the vacuum system was ∼5 $\times 10^{-11}$ Torr.

III. RESULTS AND DISCUSSION

A. Model

As a basis for discussion we review here the details of the Ps formation mechanism that we have devised to explain our measurements with positrons on silicon. First of all, we found that the fraction of the positrons implanted into a p-Si(100) surface that are emitted as Ps as a function of T can be fitted very well by assuming there are two Ps emission channels with activation energies E_a and E_b competing with annihilation of the surface positrons with rate γ. The individual emission rates are of the form

$$\Gamma_{a,b}(T) = S_{a,b}(4kT/h)\exp\{-E_{a,b}/kT\}, \qquad (5)$$

and the fractional Ps yield is

$$y(T) = y_0 + y_1 \left[\frac{\Gamma_a + \Gamma_b}{\gamma + \Gamma_a + \Gamma_b} \right]$$
$$= y_0 + y_1[1 + (g_a + g_b)^{-1}]^{-1}, \qquad (6)$$

as outlined in Ref. 64. However, this model cannot be correct because the activation energies should be dependent on the Fermi energy, which changes by about 0.2 eV over the temperature range of interest. Furthermore, the measured Ps emission energy is not proportional to the temperature,[12] as one would expect for the usual sort of thermally activated emission. Indeed, in some cases we find that the Ps emission energy *decreases* when the temperature is increased.

Our data thus demand that we seek a mechanism whereby Ps is emitted at a fixed energy from a state that is populated at a rate proportional to a Boltzmann factor with an activation energy that has no reference to the Fermi level. This requires that the state that is the parent of the emitted Ps does not exist prior to the arrival of the thermalized positron back at the surface following implantation, and that once the state exists it begins to be populated at a rate proportional to a Boltzmann factor containing an activation energy given only by the difference in the electron energy in the new state versus the prior state. The new state containing both an electron and a positron with a transient existence on the surface is posited to be a surface excitonlike object formed from a surface electron bound to a surface positron. Since the Ps emission energy is observed to have no dependence on temperature for p-Si (and an inverse dependence for n-Si and n-Ge), the surface excitonic Ps, which we denote PsX, must be metastable relative to emission as vacuum Ps.

In Table I we list the approximated positron and experimentally determined electron energy levels in or on p-Si(100) in boldface type. Given in lightface type are the positronium energies that would result from forming vacuum Ps from various pairs of electron and positron states. Negative Ps energies signify that Ps formation cannot occur spontaneously via such a channel, but must be thermally activated if it is to occur at all. X stands for the electronic surface exciton, CBM is the conduction band minimum, VBM is the valence band

TABLE I. Known and estimated single-particle energy levels (boldface entries) of positron and electron states in or on p-Si(100) in eV, referenced to the vacuum level (Vac), and Ps emission energies (lightface entries) one would expect due to combinations of various pairs of electron and positron states at 300 K. Errors are estimated to be about one unit in the last digit. The positron surface energy consistent with our measurements is an estimate differing by about 0.5 eV from the -2.0 eV calculated by Fazleev *et al.* (Ref. 67). The bulk positron energy is an estimate from a reinterpretation of the measurement of Ref. 66 as stated in the text. The electron energies are all from Kutschera *et al.*, Ref. 65. The Ps emission energies are simply the negative of the Ps binding energy, 6.803 eV, plus the sum of the contributing electron and positron energies. CBM and VBM are the conduction and valence band edges at the top and bottom of the energy gap; D_{down} and D_{up} are the empty and filled dangling-bond surface state energies; X is the electronic surface exciton level at near midgap. The Ps energy entries labelled A, B, and C are described in the text.

			Electron states					
			Vac	**CBM**	$D_{\textbf{down}}$	X	**VBM**	$D_{\textbf{up}}$
			0	**−3.67**	**−4.76**	**−0.92**	**−5.4**	**−5.5**
Positron	**Vac**	**0**	6.8	3.13	2.04	1.91	1.4	1.3
states	**Bulk**	**−0.5**	6.3	2.63	1.54	1.41	A 0.9	0.8
	Surf	**−1.5**	5.3	1.63	0.54	0.41	B −0.1	C −0.2

maximum, and D_{up} and D_{down} are the surface dangling bonds that are respectively normally below the VBM and therefore filled, and above midgap, and therefore normally empty for p-Si(100). Entry A represents the maximum energy for direct Ps emission for bulk positrons tunneling through the surface, which is energetically possible, but evidently rare; B and C are the activation energies for thermal desorption of surface positrons as positronium, with C being the most likely pathway due to the better overlap of the D_{up} dangling-bond electrons with surface positrons. The other light face areas represent numerous other branches that are not likely to be observed. The electronic energies are from Kutschera *et al.*,[65] the surface positron energy relative to the vacuum, -1.5 eV, is determined from the measured thermal activation energy $E_a = 0.2$ eV, and confirmed by the measured Ps emission energy as discussed below. The bulk positron energy relative to the vacuum (which is the opposite of the work function) is an estimate arrived at by supposing that the first reported measurement of the positron work function for Si(100), -1.0 ± 0.2 eV,[66] was actually reporting the energy spread of epithermal positrons and not signifying that the positron affinity for Si is negative.

All f_d data in this section include an $\sim$4% background that has not been subtracted, so as to facilitate comparison with Fig. 2. Unless otherwise stated, the high-voltage buncher was on for all data shown, meaning that the pulse width was $\sim$1 ns and the beam energy was at least 0.75 keV. For all data in which no error bars are shown, they are smaller than the symbols used. The p-Si data shown here were taken with the same sample used in Refs. 35 and 38. We have obtained similar data with two other p-Si samples, one cleaned in the same manner (dipping), and one that was cleaned using a pipette, as described in Sec. II D. The latter sample exhibited a slightly higher yield at room temperature, but was qualitatively the same as the "dipped" samples. No significant differences were observed between the two samples cleaned in the same way.

B. Ps yield

Figure 4(a) shows the Ps yield (i.e., f_d) from p-Si as a function of the sample temperature. These data (which are also shown in Ref. 35) were taken without using the electrostatic buncher, and with $B_T = 0.16$T and $f_{RW} = 4$ MHz, so that the effective positron density was as low as possible. We fitted these data to an Arrhenius thermal activation function[64] of the form

$$f_d = f_0 + f_1/[1 + (\gamma_s/r_A) \exp\{E_A/kT\}], \quad (7)$$

in accordance with Eq. (5). Here γ_s is the surface positron annihilation rate [1.46 ns^{-1} Ref. 67)], r_A is a temperature-independent effective attempt frequency for the process, and f_0 and f_0+f_1 are the minimum and maximum Ps fractions, respectively. The fit yields an activation energy $E_A = 0.253 \pm 0.004$ eV. Our interpretation of this measurement is that the surface positronic excitonlike energy level can be reached by a thermal fluctuation of 0.25 eV starting from an electron at the valence band maximum (with energy -5.4 eV) combining with a surface state positron (energy -1.5 eV). The PsX state then has an energy E_{PsX} relative to vacuum Ps, which is the sum of the latter three energies plus the 6.80 eV vacuum
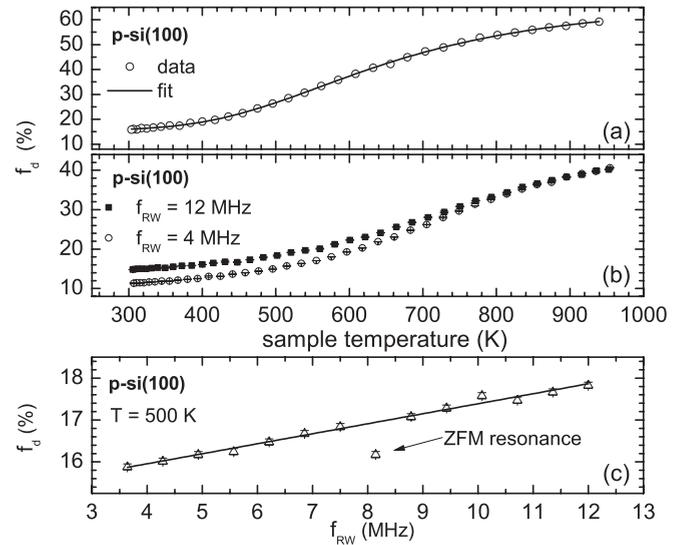
FIG. 4. Ps yield as a function of temperature using a low- (a) and high- (b) density positron beam. The solid line in (a) is a fit to an Arrhenius activation function [Eq. (8)] as described in the text. The magnetic field was 0.16 T for (a) and 2.3 T for (b) and (c). The positron beam energy is 0.75 kV with the buncher (b) and (c) and 200 V without it (a). The Ps yield vs the RW drive frequency is shown in (c), including a linear fit that does not include the point at 8.1 MHz.

Ps energy, $E_{PsX} = 6.80 + 0.25 - 5.40 - 1.5 = 0.15$eV, in agreement with our measured Ps emission energies.[35,38]

In the case of p-Si, we also observe a beam density dependence of f_d, as shown in Fig. 4(b). This occurs because for p-Si the production of e-h pairs by the beam itself can populate the D_d states and hence also the PsX state. This effect was observed more dramatically using laser irradiation,[38] where it is much easier to increase the number of e-h pairs produced. However, the implantation of positrons will also generate some e-h pairs, and if the positron beam density is high enough, e-h pair production by one positron may increase the probability that another positron is emitted as a Ps atom, leading to a linear relationship between f_{RW} and f_d, which we indeed observe in Fig. 4(c). This figure shows the Ps yield as a function of the RW drive frequency as well as a linear fit, excluding the 8.1 MHz point, which is due to a zero frequency mode plasma resonance that causes a loss of plasma density.[49,51]

The reason why the maximum yield in Fig. 4(a) is larger than that of Fig. 4(b) is that the higher magnetic field that is required for attaining a high positron density leads to magnetic quenching of positronium.[68] This effect, which will not affect f_d after around 0.75 T,[69] reduces the amount of long-lived Ps present by mixing $m = 0$ triplet and singlet states.[70] However, increasing the magnetic field also increases the positron beam density, and the increased Ps yield due to e-h pair production partially compensates for the magnetic quenching, otherwise the difference in delayed fractions would be around 40%.[54,71]

Figure 5 shows the Ps yield as a function of temperature for the n-Ge (a) and n-Si (b) samples. After the n-Ge sample was placed in the vacuum system, the room temperature value of
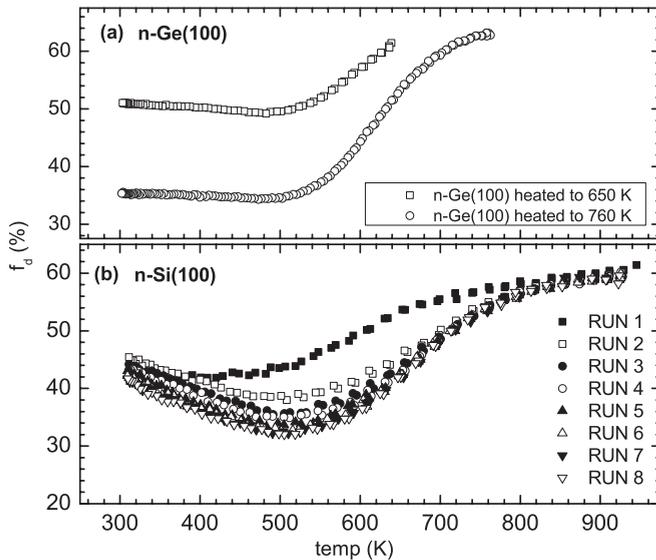
FIG. 5. Temperature scans for n-Ge(100) (a) and n-Si(100) (b). For Ge we saw two different regimes, with a drastic change after heating above 650 K. The change in the Ps yield from n-Si as it was heated is shown in the different sequential runs wherein the sample was heated to $\sim$950 K and then the temperature gradually lowered after every two positron pulses. The data in (b) do not have assigned error bars.

f_d was less than 10%. After initially heating it to $\sim$650 K for 10 min, we obtained yield curves as shown in Fig. 5(a) (open squares) with a large increase in the Ps yield. It is known that all of the chlorides on a Ge surface left after an HCl etch will be removed after annealing at 637 K for 30 min.[62] However, after further heating the temperature dependence of the Ps yield changed again, to that shown by the open circles in Fig. 5(a). After this the sample was stable (until it was irradiated with laser light, which we will discuss in the next section). The reason for this apparent transition between two distinct regimes is not presently known, but is likely to be related to the surface condition, via either contamination or structure. In both modes we observe a slight initial decrease in f_d as the sample is heated.

Thermal activation curves for n-Si are shown in Fig. 5(b). The series of curves shown highlight the thermal desorption process and show how the Ps yield changed gradually as the sample was repeatedly cycled through the heating process. Eventually the curves converge and then are generally similar to those obtained using p-Si at temperatures above $\sim$600 K. However, at lower temperatures we find that the yield is initially decreasing as the temperature is increased, just as with the n-Ge, but to a much greater extent. We believe that this is related to the diffusion of positrons back to the surface. It is known that in n-doped materials the internal near-surface electric field, which is of such a sign as to attract positrons toward the surface, will depend on the temperature and thus the effective diffusion coefficient[72] of positrons in such materials should also depend on the temperature beyond the usual temperature dependence dictated by the acoustic phonon scattering rate, even in the absence of thermally generated defects or other trapping sites.[73] Temperature-dependent positron diffusion in Si(100), and also Si(111), has
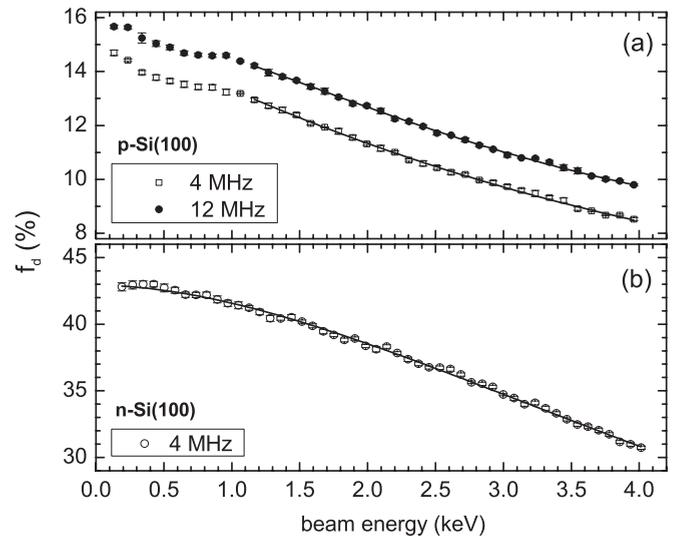
FIG. 6. Delayed fraction as a function of energy for p-Si at two different beam densities (a) and n-Si (b). The magnetic field was 0.16 T and the temperature was 300 K for these data. The solid lines are fits to Eq. (8) and do not include data for energies below 1.15 keV in (a). The high-voltage buncher was not used for these measurements.

been observed before,[74] and it was found that heating the target initially decreased the positron diffusion to the surface. This effect was attributed to the temperature dependence of the internal electric fields which affect the positron diffusion.

The extent to which f_d initially decreases in Fig. 5(b) is reduced if the high-voltage buncher is not used. Since in this case the positrons are implanted closer to the surface, this supports the idea that it is positron diffusion against a near-surface electric field rather than Ps formation behind the effect. We note also that the properly cleaned (i.e., not dipped) p-Si sample also exhibited this type of behavior, to about the same extent as the Ge.

The low-temperature yield of n-Si (diffusion-related effects notwithstanding) is much higher than was observed for p-Si. This is what one would expect based on the model of Ps formation via the PsX state.[35] For the n-doped sample the Fermi level is above the D_d level so these states, which are effective in populating PsX, are always filled, and hence the amount of Ps produced at room temperature is much higher. A similar argument applies to the n-Ge.

We have not attempted to fit a thermal activation yield to any of the data in Fig. 5 as the model implied by Eq. (7) does not apply. In addition to the temperature-dependent diffusion coefficient, occupation of the PsX state may occur via numerous channels that have a complicated interdependence. The general form of the data, however, does seem to indicate that some sort of thermal activation is taking place.

The production of e-h pairs by the incident positron beam will depend not only on the beam density but, even in the single-particle limit (i.e., for low beam density), also on the beam energy. This is evidenced in the data of Fig. 6(a), which shows the Ps yield vs the incident beam energy for p-Si. These data are taken at low magnetic field and without the buncher, and yet we can still observe that the RW compression affects f_d. This indicates not only that e-h pairs produced by the

positron beam are involved in Ps formation, but that they are able to travel a considerable distance in the Si sample (otherwise there would be no effect at low B fields). Given the nonlinear dependence of the positron penetration depth on positron implantation energy, it is curious that the 4 MHz and 12 MHz curves differ by a constant over the entire range of beam energies.

As the beam energy K is increased, the mean positron implantation depth[39] increases roughly as K^ν (with K in keV and $\nu \sim 1.7$), while the number of e-h pairs produced increases approximately linearly with the energy. Thus, there will initially be two competing effects, an increased number of e-h pairs produced in an increasing volume. The electron density at the surface will then depend on these factors as well as on the electron diffusion to and at the surface. The interplay between the e-h production, density, and diffusion is presumably the cause behind a plateau in the yield versus energy curve shown in Fig. 6(a). Although the simple idea of increasing production and decreasing density can explain the effect qualitatively, the real situation is undoubtedly more complex, and we have not yet been able to produce a model that properly describes the data in Fig. 6(a); the sharp transition from the plateau region to the monotonically decreasing yield does not fit with any simple model and may indicate that additional processes are occurring. It is interesting to note that a hint of the structure seen in Fig. 6(a) is present in Fig. 2(a) of Ref. 74 [where a Si (100) target was used].

In addition to the surface electron density, the Ps fraction will also depend on positron diffusion back to the surface, which is described by

$$f_d = f_0[1 + (K/K_0)^\nu]^{-1}, \qquad (8)$$

where K_0 is the implantation energy at which half of the positrons implanted are able return to the surface[75] and f_0 is the branching ratio for Ps formation. A typical value for ν is around 1.7,[39,76] although it is known to be somewhat sample dependent. This model, however, may not apply to semiconductors in which the beam energy can affect the e-h pair density, and hence f_0. Nevertheless, we have fitted Eq. (8) to our data to obtain rough estimates of the half-energy K_0. In general we find that if ν is allowed to vary as a free parameter our fits tend to favor values between 1.2 and 1.6, perhaps indicating the inapplicability of the model in general to these kinds of samples. However, the value of K_0 obtained is fairly insensitive to such variations. For example, with the n-Ge sample we obtain $K_0 \sim 7$ keV with ν optimized at 1.2 (that is, if it is a free parameter in the fit). If, however, ν is held constant at 1.7 we find $K_0 = 6.8$ keV, with a degraded fit quality. Our fits for p-Si and n-Si [shown in Figs. 6(a) and 6(b), respectively] indicate $K_0 \sim 4$ and 6 keV, respectively, although these numbers should not be taken too seriously when K_0 is obviously much greater than the highest positron energy used in the measurement, and when the fitted function is clearly inadequate. Aside from the possibility of e-h pair formation contributing to the Ps yield, one of the main problems with using the model implied by Eq. (8) to obtain K_0 from semiconductors is that, as mentioned above, there may be internal electric fields that affect the effective positron diffusion coefficient (see Fig. 5).
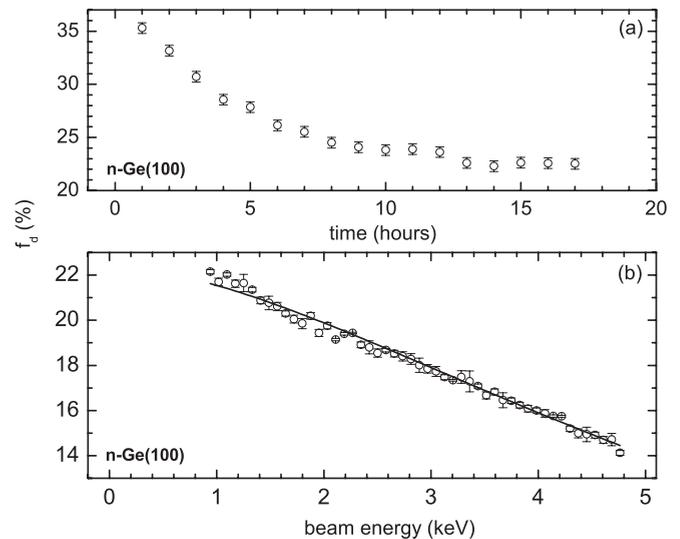

FIG. 7. Decay of f_d from n-Ge with time (a) and energy scan taken after decay (b). The beam energy for the time scan in (a) was 0.94 keV.

Our measurements of $f_d(K)$ for n-Ge are shown in Fig. 7. Unfortunately this sample was not stable during the measurements. The exact reason for this is unknown, but it may be due to laser damage induced prior to the measurement. Figure 7(a) shows the declining value of f_d for the lowest beam energy (0.94 keV) with time. By averaging over some of the later measurements (when the rate of decay had slowed down) we obtain, by fitting to Eq. (8), an approximate value of $K_0 \sim 7$ keV for this sample, shown in Fig. 7(b). The laser power that may have created damage, or otherwise affected the surface of the n-Ge sample, was $\sim$30 mJ/pulse over an area of $\sim$0.2 cm^2. Similar light pulses had no effect on n-Si, and actually gave rise to a large photoemission yield from p-Si, without generating any significant damage.[38] We do not presently understand why Ge would be more susceptible to such damage than Si. It may be related to different types of impurities or the particular characteristics of the surfaces. More work is required to explain this observation, but we can conclude that n-Ge samples similar to that used here may not be suitable for photoemission experiments, or as a source of photoemitted Ps atoms for other experiments.

C. Ps energy

We measure the energy of the emitted Ps via the Doppler width (or shift) of the $1S$-$2P$ transition. (The general methods used to excite and detect this transition are described in Refs. 26 and 29.) We may do so with the laser either parallel to the sample surface or directed into the target, which allows us to determine both the parallel and perpendicular Ps energy, as explained in Ref. 35. Our previous measurements on p-Si showed that the energy of Ps emitted via the PsX state has a constant value of $\sim$0.16 eV, whether it is produced by thermal activation[35] or laser irradiation.[38] For this sample, the PsX component of the total Ps yield is fairly small at low temperatures ($\sim$10%), and the Ps energy *appears* to decrease as the temperature is increased. However, if the fast and slow components are decoupled it may be seen that this is simply
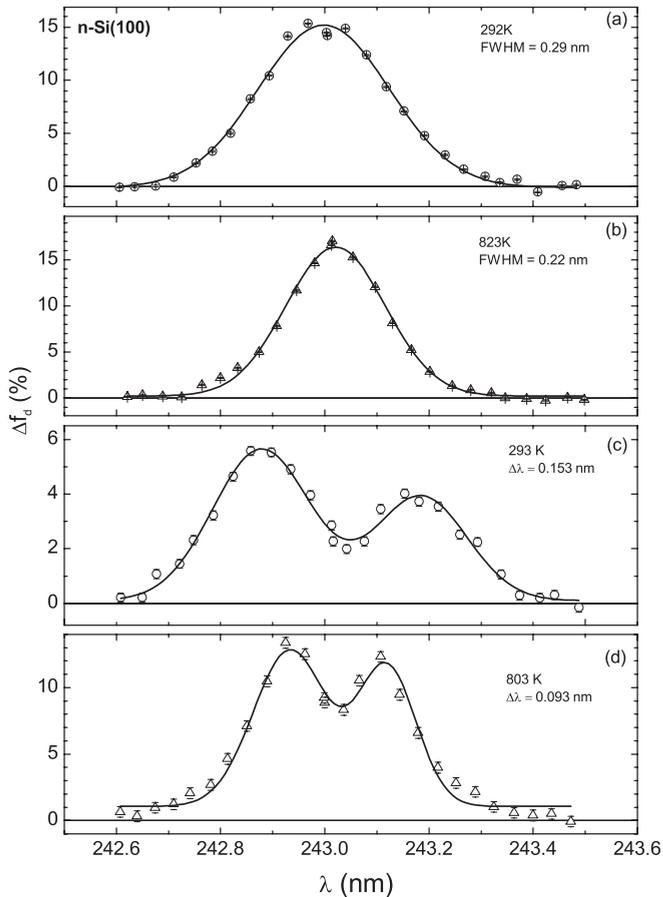
FIG. 8. Laser spectroscopy of Ps using n-Si(100), showing parallel (a) and (b) and perpendicular (c) and (d) Doppler measurements.

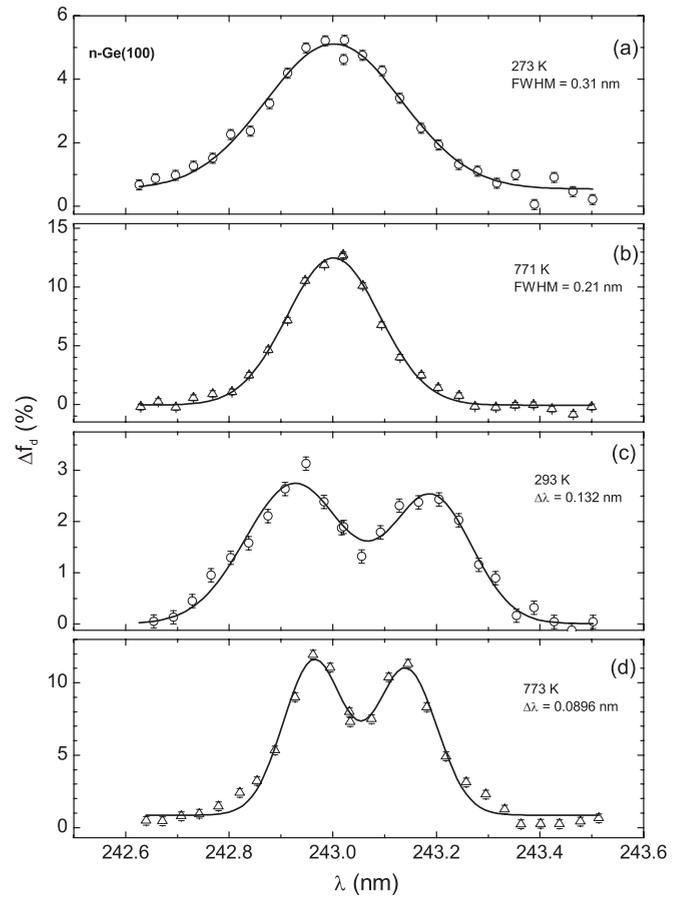FIG. 9. Laser spectroscopy of Ps using n-Ge(100), showing parallel (a) and (b) and perpendicular (c) and (d) Doppler measurements.

due to the contribution from direct Ps formation, which does not depend on the temperature. For n-Si and n-Ge, the situation is rather different; even at room temperature the PsX yield is the dominant component, and the fast component is always negligible. Thus, for these samples, changes in the Doppler profiles actually do reflect changes in the PsX energy.

Figure 8 shows parallel and perpendicular Doppler profiles measured for n-Si. These have been fitted to Gaussian or double Gaussian functions; although this provides a convenient way to characterize the data, it is not, strictly speaking, correct as we do not have thermal distributions, but rather line shapes determined, we presume, mostly by the (unknown) Ps angular distribution. The fit is clearly inadequate in the wings of the double Gauss plots. However, a comparison of the energy values inferred from such fits with a calculation of the root mean square mean wavelength deviation (as was used in Ref. 35) leads only to a correction of the order of 10%. We convert the Doppler width or shift σ to Ps energy using

$$\sigma^2 \left[\frac{c}{\lambda_0} \right]^2 \frac{m_e}{e} = [\sigma^2 \text{ (nm)}] \times 8.654 = E \text{ (eV)}, \qquad (9)$$

where $\lambda_0 = 243$ nm and the other symbols have the usual meanings. The parallel Doppler profiles in Fig. 8 indicate that the Ps energy changes from 131 to 75 meV when the sample temperature is changed from 292 to 823 K. Similarly, the Doppler shifts of the perpendicular data in the same figure

suggest that these energies change from 203 to 75 meV for a similar temperature change of the target. These values are always higher than thermal, which is to be expected for Ps produced via a nonthermal mechanism. The surprising result that heating the target actually reduces the Ps energy would seem to indicate that the surface energy levels depend on the sample temperature, most likely via the electronic population of surface states.

We note that the center of the double dip in Figs. 8(c) and 8(d) is slightly offset from the centroid position of the parallel measurements (i.e., 243 nm). This is due to the alignment of the target and laser beams but does not affect our determination of the Doppler shift, which will still be given by half of the separation of the two peaks.

Figure 9 shows that the n-Ge sample exhibits a similar effect to that observed with the n-Si sample, with the parallel energy changing from 151 to 70 meV when the sample is heated from room temperature to 771 K, and the perpendicular energy changing from 151 to 69 meV when the sample is heated by a similar amount. We note that the n-Ge data were taken *after* the sample had been heated to 760 K (see Fig. 5). We attribute the (negative) temperature dependence of the Ps energy in both n-Si(100) and n-Ge(100) to changes in the surface energy levels, and thus to the energy of the PsX state with respect to the vacuum; when the samples are hot the D_{down} states are highly populated with electrons, and we speculate that the presence of so much charge on the surface changes the energy levels. It
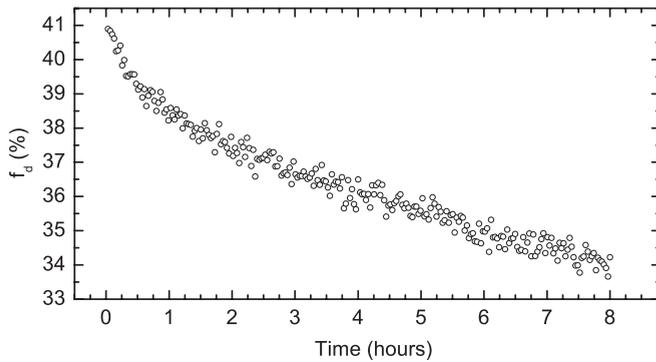
FIG. 10. Ps yield from p-Si(100) after laser irradiation with no heating, demonstrating laser desorption of surface hydrogen.

would be interesting to check this hypothesis in photoemission experiments by measuring the energy of emitted electrons from this state as a function of the sample temperature.

D. Surface preparation by laser irradiation

For all of the experiments described so far the samples were first heated to desorb hydrogen (or, for Ge, chloride) layers. These layers serve to protect the sample surfaces while it is transferred to the vacuum system after cleaning, but must be removed before measurements can be made. In some circumstances it may not be convenient (or possible) to heat a sample *in situ*. For example, most closed-cycle helium expanders (which are used to cool samples to cryogenic temperatures) cannot be heated above $\sim$350 K, so studies of Ps emission from a cold surface would benefit from using laser desorption instead of heating.

We investigated the possibility of laser desorption of the hydrogen from a p-Si sample. When the sample was first installed into the vacuum system we measured $f_d \sim 6\%$. After irradiation of the sample with ten shots of $\sim$200 mJ/cm^2 of green light (532 nm), f_d increased to over 40%, but then began to decay with time, as shown in Fig. 10. After 19 h f_d had fallen to $\sim$31% but showed no signs of stabilizing. Subsequent heating of this sample returned it to the same state as was observed with other p-Si(100) samples that had not been irradiated. Figure 10 is strikingly different from Fig. 4, in which $f_d \sim 15\%$ at room temperature for p-Si. The much higher Ps yield seen in Fig. 10, despite the decay, indicates that laser irradiation has made some sort of structural change to the target. One possibility is that, following the laser irradiation, hydrogen has been desorbed, but the surface is not the (2×1) reconstructed surface usually obtained after heating. The long relaxation could then be the slow rearrangement of surface bonds, which evidently are in a metastable state following the laser irradiation. Laser-induced structural modifications of this type could be studied by performing low-energy electron diffraction measurements before and after laser irradiation.

IV. SUMMARY AND CONCLUSIONS

Although positronium formation from silicon surfaces has been studied before many times,[37,74] without measuring both the Ps yield and energy as a function of temperature there

was no way to recognize that the Ps formation mechanism is actually rather different from other known processes. That is, the thermal desorption data look exactly like a thermal activation process, because that is in fact what it is; unlike in the case of metals though, here it is electrons that are thermally activated to positron-induced surface electronic states and not the surface electron-positron pairs that are desorbed as Ps atoms. Similarly, the constant Ps energy could be mistaken for a "direct" Ps formation process, even though the actual energy is significantly lower than the 1–2 eV that is typically found for this type of Ps coming from a metal surface.

Our initial experiments have shown that Ps formation on p-Si(100) takes place via a different mechanism involving a positron surface state that seems to be a type of exciton,[35] and that electrons may be promoted to this state by laser irradiation, resulting in what may be described as the photoemission of Ps.[38] The follow-up measurements presented here have provided additional information which we summarize as follows:(1) Electron-hole pairs produced by the incident positron beam itself can augment the amount of Ps produced in p-Si.(2) The room temperature Ps yield from n-Si (and n-Ge) is higher than that from p-Si.(3) The energy of Ps emitted from p-Si, n-Si, and n-Ge is not thermal and is very similar from all samples studied (of the order of 150 meV at 300 K).(4) The Ps energy from both n-Si and n-Ge decreases by a factor of 2 when the samples are heated, in contrast to p-Si, for which the energy does not depend on the sample temperature.(5) Unlike the large photoemission yield of Ps caused in p-Si, electron-hole production by laser irradiation has a negligible effect on the Ps yield from n-Si but leads to a small increase in the yield from n-Ge, as well as apparently causing some sample damage.(6) Hydrogen may be desorbed from the surface by laser irradiation of p-Si, resulting in a high yield of Ps without heating.(7) Laser desorption of hydrogen also appears to produce metastable structural changes of the surface of p-Si that dramatically increase the Ps yield.

The fact that the positron beam itself may be used to produce Ps via the production of e-h pairs supports our model and rules out any (unknown) laser effects that could perhaps have given rise to the Ps we observe. Indeed, the observations listed above are generally consistent with our model of Ps formation via a surface exciton state,[35] although some aspects of our data suggest that the situation may be more complicated. For example, in our model the D_{down} states should be filled for n-type samples, and so we might expect that they would exhibit the maximum Ps yield at any temperature. Although the room temperature yields are relatively high (with respect to p-Si), there is obviously still some temperature dependence for the n-type samples (as shown in Fig. 5). This could be related to the observation that the Ps emission energy also depends on the sample temperature; since Ps formation is in competition with the positron surface state lifetime, any changes that affect the PsX energy level may also affect the Ps formation rate and hence the yield.

A number of important measurements remain to be done. Our sample preparation methods are relatively simple, and more elaborate procedures might result in cleaner surfaces. Elucidation of the roles played by surface impurities in

determining electronic and PsX energy levels, as well as scattering effects during Ps emission, should help clarify the basic mechanisms occurring and may suggest ways to control the characteristics of the emitted Ps.

We have attributed the observed Ps energy spread (from all samples) to scattering during the emission process. This is only speculation, but is supported by the observation that the reduced emission energy from the hot n-type samples also leads to a reduced energy spread. If Ps emitted from a cold and/or perfectly cleaned sample should turn out to be very monoenergetic, such Ps would be more amenable to laser excitation owing to the reduced Doppler spread. Note that the fact that the Ps would still be emitted with ~150 meV just means that an excitation laser would have to be detuned from the resonant frequency accordingly; the efficiency of excitation will increase so long as there is a decreased Doppler width.

It would be informative to systematically study the Ps yield and energy obtained from different samples and for varying doping levels. Other elemental and compound semiconductors that have dangling-bond states should produce Ps via the same basic mechanism, and by varying their properties it may be possible to adjust the Ps energy. An efficient source of cold Ps that may be used in a low-temperature environment, and that allows for the production of short-time bursts of positronium atoms,[77] could have numerous experimental applications, including direct Ps gravity measurements,[78] the formation of antihydrogen atoms via Ps-antiproton interactions,[79] Ps-atom scattering,[7] loading of a stellarator to study electron-positron plasmas,[80] the production of positron-atom bound states,[81] and precision laser spectroscopy.[4,82] Any type of experiment involving Ps-laser interactions would benefit from an efficient source of monoenergetic Ps, since the Doppler spread of these light atoms (~500 GHz for thermal Ps) is in general much larger than typical laser bandwidths and is the limiting factor in the excitation efficiency.

It has not been experimentally verified that very low-temperature samples will photoproduce Ps efficiently.[38] In the case of Si, the surface reconstruction changes from (2×1) to (4×2) below ~150 K;[83] while we might not expect this to significantly affect the formation of Ps it should be checked, especially since the electronic surface exciton observed by Wienelt *et al.*[36] was only observed for the (4×2) surface.[84] If there were a thermal contribution to the energy spread of emitted Ps, then photoemission from a cold target would provide a narrow beam. Furthermore, some experiments require that the target be cold (e.g., Ref. 79).

We have measured positronium emission from both p- and n-type Si(100) and from (lightly doped) n-type Ge(100). Our data support the idea that Ps from these materials is mostly produced via an excitonlike surface state. For n-type samples, the spontaneous Ps yield is quite high ($f_{Ps} > 80\%$) at room temperature, and the Ps energy decreases with increasing temperature. We attribute this to changes in the dangling-bond energy levels due to a large amount of thermally generated charge on the surface. This observation suggests that it may be possible to tune the Ps emission energy via the target material properties, so that colder Ps might be produced for any target temperature. We expect Ps produced by this mechanism to be useful for a wide variety of experiments.

[1] S. Berko and H. N. Pendleton, Annu. Rev. Nucl. Part. Sci. **30**, 543 (1980).

[2] A. Rich, Rev. Mod. Phys. **53**, 127 (1981).

[3] R. Ley, Appl. Surf. Sci, **194**, 301 (2002).

[4] For example, M. S. Fee, A. P. Mills, S. Chu, E. D. Shaw, K. Danzmann, R. J. Chichester, and D. M. Zuckerman, Phys. Rev. Lett. **70**, 1397 (1993); S. Chu, A. P. Mills, and J. L. Hall, *ibid.* **52**, 1689 (1984).

[5] A. P. Mills Jr., Phys. Rev. Lett. **46**, 717 (1981); F. Fleischer, K. Degreif, G. Gwinner, M. Lestinsky, V. Liechtenstein, F. Plenge, D. Schwalm, *ibid.* **96**, 063401 (2006); K. Michishio, T. Tachibana, H. Terabe, A. Igarashi, K. Wada, T. Kuga, A. Yagishita, T. Hyodo, and Y. Nagashima, *ibid.* **106**, 153401 (2011).

[6] D. B. Cassidy and A. P. Mills Jr., Nature (London) **449**, 195 (2007).

[7] G. Laricchia, S. Armitage, A. Kover, and D. J. Murtagh, Adv. At., Mol., and Opt. Phys. **56**, 1 (2008).

[8] K. G. Lynn, Phys. Rev. Lett. **43**, 391 (1979).

[9] L. Xie, G. B. DeMaggio, W. E. Frieze, J. DeVries, D. W. Gidley, H. A. Hristov, and A. F. Yee, Phys. Rev. Lett. **74**, 4947 (1995).

[10] D. W. Gidley, A. R. Köymen, and T. W. Capehart, Phys. Rev. Lett. **49**, 1779 (1982).

[11] A. P. Mills Jr., L. Pfeiffer, and P. M. Platzman, Phys. Rev. Lett. **51**, 1085 (1983).

[12] A. P. Mills Jr. *et al.*, Phys. Rev. Lett. **66**, 735 (1991).

[13] T. Yamazaki, T. Namba, S. Asai, and T. Kobayashi, Phys. Rev. Lett. **104**, 083401 (2010).

[14] Martin Deutsch, Phys. Rev. **82**, 455 (1951).

[15] M. H. Weber, S. Tang, S. Berko, B. L. Brown, K. F. Canter, K. G. Lynn, A. P. Mills Jr., L. O. Roellig, and A. J. Viescas, Phys. Rev. Lett. **61**, 2542 (1988).

[16] K. F. Canter, A. P. Mills Jr., and S. Berko, Phys. Rev. Lett. **33**, 7 (1974).

[17] P. J. Schultz and K. G. Lynn, Rev. Mod. Phys. **60**, 701 (1988).

[18] M. J. Puska and R. M. Nieminen, Rev. Mod. Phys. **66**, 841 (1994).

[19] A. Greenberger, A. P. Mills Jr., A. Thompson, and S. Berko, Phys. Lett. A **32**, 72 (1970).

[20] Y. Nagashima, Y. Morinaka, T. Kurihara, Y. Nagai, T. Hyodo, T. Shidara, and K. Nakahara, Phys. Rev. B **58**, 12676 (1998).

[21] J. Callaway, Phys. Rev. **116**, 1140 (1959).

[22] A. P. Mills Jr., G. R. Brandes, D. M. Zuckerman, Weimin Liu, and S. Berko, Mater. Sci. Forum **105-110**, 763 (1992).

[23] A. P. Mills Jr., in *Positron Spectroscopy of Solids*, edited by A. Dupasquier and A. P. Mills Jr. (IOS Press, Amsterdam, 1995), p. 181.

[24] A. P. Mills Jr. and L. Pfeiffer, Phys. Rev. Lett. **43**, 1961 (1979).

[25] E.g., Y. Kobayashi, K. Ito, T. Oka, and K. Hirata, Radiat. Phys. Chem. **76**, 224 (2007).

[26] D. B. Cassidy, P. Crivelli, T. H. Hisakado, L. Liszkay, V. E. Meligne, P. Perez, H. W. K. Tom, and A. P. Mills Jr., Phys. Rev. A **81**, 012715 (2010).

[27] P. Crivelli, U. Gendotti, A. Rubbia, L. Liszkay, P. Perez, and C. Corbel, Phys. Rev. A **81**, 052703 (2010).

[28] Oxidized channels in Si may also be used. Although these materials are not porous, they exhibit positronium formation and cooling mechanisms that are essentially the same as those observed in porous films. S. Mariazzi, P. Bettotti, S. Larcheri, L. Toniutti, and R. S. Brusa, Phys. Rev. B **81**, 235418 (2010).

[29] D. B. Cassidy, T. H. Hisakado, V. E. Meligne, H. W. K. Tom, and A. P. Mills Jr., Phys. Rev. A **82**, 052511 (2010).

[30] D. W. Gidley, W. E. Frieze, T. L. Dull, A. F. Yee, E. T. Ryan, and H.-M. Ho, Phys. Rev. B **60**, R5157 (1999).

[31] By "damage" we mean here anything that can reduce either the amount of Ps produced or its subsequent lifetime [D. B. Cassidy, K. T. Yokoyama, S. H. M. Deng, D. L. Griscom, H. Miyadera, H. W. K. Tom, C. M. Varma, and A. P. Mills, Phys. Rev. B **75**, 085415 (2007)]; in general, the physical structure of the samples is not affected by radiation.

[32] H. Saito and T. Hyodo, Phys. Rev. B **60**, 11070 (1999).

[33] D. B. Cassidy and A. P. Mills Jr., Nucl. Instrum. Methods Phys. Res., Sect. B **262**, 59 (2007).

[34] D. B. Cassidy, S. H. M. Deng, R. G. Greaves, and A. P. Mills Jr., Rev. Sci. Instrum. **77**, 073106 (2006).

[35] D. B. Cassidy, T. H. Hisakado, H. W. K. Tom, and A. P. Mills Jr., Phys. Rev. Lett. **106**, 133401 (2011).

[36] M. Weinelt, M. Kutschera, T. Fauster, and M. Rohlfing, Phys. Rev. Lett. **92**, 126801 (2004).

[37] A. P. Mills Jr., Solid State Commun. **31**, 623 (1979).

[38] D. B. Cassidy, T. H. Hisakado, H. W. K. Tom, and A. P. Mills Jr., Phys. Rev. Lett. **107**, 033401 (2011).

[39] A. P. Mills Jr. and R. J. Wilson, Phys. Rev. A **26**, 490 (1982).

[40] J. Algers, P. Sperr, W. Egger, G. Kögel and F. H. J. Maurer, Phys. Rev. B **67**, 125404 (2003).

[41] A. P. Mills Jr. and E. M. Gullikson, Appl. Phys. Lett. **49** 1121 (1986).

[42] *Positron Beams and Their Applications*, edited by P. Coleman (World Scientific, Singapore, 1999).

[43] T. J. Murphy and C. M. Surko, Phys. Rev. A **46**, 5696 (1992).

[44] C. M. Surko and R. G. Greaves, Phys. Plasmas **11**, 2333 (2004).

[45] R. C. Davidson, *Physics of Nonneutral Plasmas* (Addison-Wesley, Redwood City, CA, 1990).

[46] F. Anderegg, E. M. Hollmann and C. F. Driscoll, Phys. Rev. Lett. **81**, 4875 (1998).

[47] R. G. Greaves and C. M. Surko, Phys. Rev. Lett. **85**, 1883 (2000).

[48] D. H. E. Dubin and T. M. O'Neil, Rev. Mod. Phys. **71**, 87 (1999).

[49] J. R. Danielson and C. M. Surko, Phys. Rev. Lett. **94**, 035001 (2005).

[50] J. R. Danielson, C. M. Surko, and T. M. O'Neil, Phys. Rev. Lett. **99**, 135005 (2007).

[51] D. B. Cassidy, R. G. Greaves, V. E. Meligne and A. P. Mills Jr., Appl. Phys. Lett. **96**, 101502 (2010).

[52] R. G. Greaves and J. M. Moxom, Phys. Plasmas **15**, 072304 (2008).

[53] C. M. Surko, in *Physics with Many Positrons*, edited by R. S. Brusa, A. Dupasquier, and A. P. Mills Jr. (North-Holland, Amsterdam, 2010).

[54] D. B. Cassidy, in *Physics with Many Positrons* (Ref. 53).

[55] D. B. Cassidy and A. P. Mills Jr., Nucl. Instrum. Methods Phys. Res., Sect. A **580**, 1338 (2007).

[56] D. B. Cassidy *et al.*, Appl. Phys. Lett. **88**, 194105 (2006).

[57] R. M. Drisko, Phys. Rev. **102**, 1542 (1956).

[58] S. Chu and A. P. Mills Jr., Phys. Rev. Lett. **48**, 1333 (1982).

[59] H. Fritzsche, J. Phys. Chem. Solids **6**, 69 (1958).

[60] E. Yablonovitch, D. L. Allara, C. C. Chang, T. Gmitter, and T. B. Bright, Phys. Rev. Lett. **57**, 249 (1986).

[61] V. L. Thanh, D. Bouchier, and G. Hincelin, J. Appl. Phys. **87**, 3700 (2000).

[62] S. Sun, Y. Sun, Z. Liu, D-I. Lee, S. Peterson, and P. Pianetta, Appl. Phys. Lett. **88**, 21903 (2006).

[63] T. J. Grassman, S. R. Bishop, and A. C. Kummel, Surf. Sci. **602**, 2373 (2008).

[64] S. Chu, A. P. Mills Jr., and C. A. Murray, Phys. Rev. B **23**, 2060 (1981).

[65] M. Kutschera, M. Weinelt, M. Rohlfing, and T. Fauster, Appl. Phys. A **88**, 519 (2007).

[66] A. P. Mills Jr., P. M. Platzman, and B. L. Brown, Phys. Rev. Lett. **41**, 1076 (1978).

[67] N. G. Fazleev, J. L. Fry, and A. H. Weiss, Phys. Rev. B **70**, 165309 (2004).

[68] O. Halpern, Phys. Rev. **94**, 904 (1954).

[69] D. B. Cassidy, T. H. Hisakado, H. W. K. Tom, and A. P. Mills Jr., Phys. Rev. Lett. **106**, 173401 (2011).

[70] D. B. Cassidy, V. E. Meligne, and A. P. Mills Jr., Phys. Rev. Lett. **104**, 173401 (2010).

[71] R. M. Drisko, Phys. Rev. **102**, 1542 (1956).

[72] A. P. Mills Jr. and C. A. Murray, Appl. Phys. **21**, 323 (1980).

[73] For example, K. G. Lynn and H. Lutz, Phys. Rev. B **22** 4143 (1980).

[74] B. Nielsen, K. G. Lynn, A. Vehanen, and P. J. Schultz, Phys. Rev. B **32**, 2296 (1985). While the type of doping of the Si used was not stated in this paper, it was most likely *n* type [K. G. Lynn (private communication)].

[75] A. P. Mills Jr., Phys. Rev. Lett. **41**, 1828 (1978).

[76] P. Asoka-Kumar and K. G. Lynn, Appl. Phys. Lett. **57**, 1634 (1990).

[77] Various insulators are able to produce cold Ps, [e.g., S. Mariazzi, P. Bettotti, and R. S. Brusa, Phys. Rev. Lett. **104**, 243401 (2010)] but generally not in short bursts (see Ref. 29).

[78] A. P. Mills Jr. and M. Leventhal, Nucl. Instrum. Methods Phys. Res., Sect. B **192**, 102 (2002).

[79] P. Perez and A. Rosowsky, Nucl. Instrum. Methods Phys. Res., Sect. A **545**, 20 (2005); A. Kellerbauer *et al.*, (AEGIS Collaboration) Nucl. Instrum. Methods Phys. Res., Sect B **266**, 351 (2008); F. Castelli, I. Boscolo, S. Cialdi, M. G. Giammarchi, and D. Comparat, Phys. Rev. A **78**, 052512 (2008).

[80] T. S. Pedersen *et al.*, J. Phys. B **36**, 1029 (2003).

[81] E.g., D. M. Schrader, in *Physics with Many Positrons* (Ref. 53).

[82] D. B. Cassidy, H. W. K. Tom, and A. P. Mills Jr., in *Proceedings of the Workshop on Cold Antimatter Plasmas and Application to Fundamental Physics*, edited by Yasuyuki Kanai and Yasunori Yamazaki, AIP Conf. Proc. No. 1037 (AIP, Melville, NY, 2008), p. 66.

[83] R. A. Wolkow, Phys. Rev. Lett. **68**, 2636 (1992).

[84] M. Wienelt, M. Kutschera, R. Schmidt, C. Orth, T. Fauster, and M. Rohlfing, Appl. Phys. A **80**, 995 (2005).